Poor correlation between phytoplankton community growth rates and nutrient concentration in the sea

Aurore Regaudie-de-Gioux*[1], Sofía Sal, and Ángel López-Urrutia

Instituto Oceanografico Español, Avenida Principe de Asturias 70bis, 33212 Gijón, Spain.

[1] Present address: Centro de Biologia Marinha, Rodovia Manoel Hypolito do Rego km131.5, Praia do Cabelo Gordo, São Sebastiao, 11600-000, Brazil.

* Corresponding author: auroreregaudie@yahoo.fr

Abstract

Nutrient availability is one of the major factors regulating marine productivity and phytoplankton community structure. While the response of phytoplankton species to nutrient variation is relatively well known, that of phytoplankton community remains unclear. We question whether phytoplankton community growth rates respond to nutrient concentration in a similar manner to phytoplankton species composing the community, that is, following Monod's model. Data on in situ marine community growth rates in relation to nutrient concentration and the behaviour of a simple multi-species community model suggest that community growth rate does not respond to nutrient concentration according to the Monod equation. Through a simulation study we show this can be explained as a consequence of changes in size structure. Marine biogeochemical models must not parameterize phytoplankton community growth rate response to nutrient concentration usign a single Monod equation but rather involve different phytoplankton functional groups each with different equation parameters.

1. Introduction

There is little doubt that nutrient availability is one of the major factors regulating marine productivity and phytoplankton community structure. In most areas of the oceans, phytoplankton species compete for available nutrients. We know from laboratory experiments that most of the steady state growth rates of monocultures of phytoplankton species in a gradient of nutrient concentration are well represented by Monod theory (Dugdale, 1967). Small phytoplankton species have low half-saturation constants and high maximum growth rates that allow them to uptake nutrients at a faster rate than larger cells and to dominate in nutrient limited conditions (Eppley et al., 1969; Aksnes and Egge, 1991; Hein et al. 1995). Large phytoplankton species achieve slower growth rates (Grover, 1989) but often dominate when nutrient concentration is high (Tremblay and Legendre, 1994; Li, 2002) (Fig. 1). Indeed, large phytoplankton communities seem to dominate in productive ecosystems thanks to their physical and chemical capacities to escape to zooplankton grazing (Irigoien et al., 2004; Irigoien et al., 2005). Furthermore, it has been observed that large phytoplankton dominate in high turbulence regime (Rodríguez et al., 2001; Li, 2002) and that when nitrogen supply is pulsed, large cells could dominate due to their enhanced storage capacities (Litchman et al., 2009).

This leaves a scenario (Fig. 1) where nutrient-limited ecosystems are dominated by fast-growing, small phytoplankton cells, while high-nutrient environments are dominated by slow-growing, large phytoplankton species. As a result, it is possible to reach the counterintuitive result that the community growth rate (μ_{com}), i.e., the mean growth rate of the phytoplankton cells in a community, can be higher when nutrients are limited (Fig. 1). Franks (2009) contended the common practice in marine ecosystem models to parameterize phytoplankton community growth rates using Michaelis-Menten kinetics. Following our conceptual argumentation, it is indeed quite likely that the response of community growth rate is different to that of individual species.

In this study, we use a database of in situ phytoplankton community growth rate measurements in surface waters of the global ocean covering oligotrophic as well as productive ecosystems and test the hypothesis that the response of phytoplankton community growth rates to nutrient concentration does not follow Monod kinetics. We also develop a simple statistical model summarizing our conceptual framework (Fig. 1). We first parameterize, using in-situ phytoplankton size structure data (Marañon et al., 2012), the steeper phytoplankton size spectra slope when nutrient concentrations are

low. We then combine this size structure information with simple allometric equations describing the response of phytoplankton species growth to nutrients (Edwards et al., 2012) and calculate the predicted response of phytoplankton community growth rates to nutrients.

2. Methods

2.1. In situ community growth data. We used an independent dataset containing phytoplankton in situ growth rate measurements in surface waters of the ocean compiled by Chen and Liu (2010) (*see* Chen and Liu (2010) Web appendix, Table A1, http://www.aslo.org/lo/toc/vol_55/issue_3/0965a.html). We refer here to community growth rate (μ_{com}) as the specific growth rate measured in a dilution experiment which represents the average biomass-specific growth rates of the cells in a phytoplankton community. The dataset covers open ocean, coastal regions as well as High Nutrient-Low Chlorophyll (HNLC) areas and is restricted to experiments conducted in surface waters to reduce the effects of light limitation. The results described here represent the whole dataset, including HNLC. We removed from the original dataset all data for which nitrate concentration was below the detection limit or lower than 0.01 μmol L^{-1}. The database compiles data from experiments based on the dilution technique (Landry and Hassett, 1982) to estimate in situ phytoplankton community growth rate (μ_{com}, d^{-1}). Two different estimates of phytoplankton community growth rates are obtained in dilution experiments: nutrient amended or maximum growth rate (μ_{com_max}) and non-amended or growth rate (μ_{com}) under natural conditions.

If the in situ community growth rate (μ_{com}) responds to the nutrient concentration following Monod's equation, we could formulate:

$$\mu_{com} = \frac{S}{S+K_s}\mu_{com\_max} \qquad (1)$$

Where S is the nutrient concentration (e.g. nitrate, phosphate, silicate, iron and so on) and K_s is the half-saturation constant for that nutrient.

The population maximum growth rate (μ_{com_max}) is the growth rate measured when the population is not limited by nutrients and depends directly on the same parameters than the growth rate but nutrient concentration.

$$\mu_{com_{max}} = f(T, PAR, s.s., d.l., s.c., \ldots) \qquad (2)$$

Where T is the temperature, PAR is the photosynthetically active radiation, s.s. is the

species size, d.l. is the day length, and s.c. is the species composition.

Thus, the ratio μ_{com}:μ_{com_max} is a direct index of nutrient-limited growth (Brown et al. 2002), also called relative reproductive rate (μ_{com_rel}) (Sommer 1991).

$$\mu_{com_{rel}} = \frac{\mu_{com}}{\mu_{com_{max}}} \qquad \mu_{com_{rel}} = \frac{S}{S + K_s} \tag{3}$$

2.2. Community growth rate model description. We simulate the growth rate of a community under different nutrient concentrations. For that we used a database containing size structure information for 423 different phytoplankton communities (Marañon et al., 2012). For simplicity, only one nutrient (nitrogen) was considered to be limiting. In our simulations, the phytoplankton community is composed by 55 phytoplankton species ranging in cell size from 0.33 μm^3 to 5 10^5 μm^3 of volume. This size range encompasses the whole phytoplankton species size range observed in situ, from prochlorococcus size (Partensky et al., 1999) to the largest diatoms (Agustí et al., 1987). The size-abundance spectrum slope determined the relative abundance of each species. Because size spectra slope varies depending on the trophic state of the system, we empirically derived a relationship between size spectra slope and nutrient concentration (*see* subsection below). Indeed, Platt and Denman (1997) exposed the use of a property of the biomass size in that the normalized biomass is an estimate of the number of density of organisms in each size class. Although this should be considered an approximation (Blanco et al., 1994), we used the changes in scaling of normalized biomass with different nutrient levels to simulate the changes in the size scaling of the numerical abundance of species at different nutrient levels. The community growth rate is the average growth rate of all the cells within the community and is calculated as the mean growth rate of the 55 phytoplankton species weighted by the total biomass of each species. This rate is equivalent to the growth rate measured experimentally as the rate of total community in situ growth rate (μ, in the dilution dataset).

2.3. Parameterisation of the size-spectrum dependence on resource levels with in-situ size structure data. Chlorophyll *a* (Chl *a*) data for 3 different size classes (0.2-2 μm, 2-20 μm, and >20 μm) were collected from Marañon et al. (2012). As Sprules and Munawar (1986), we used the Chl *a* data to calculate the normalized biomass spectrum (NBSS) by regressing the logarithm of the normalized chlorophyll by biovolume. The biovolume was calculated using the volume equation of a sphere (Hillebrand et al.,

1999). Nutrient concentration (Σ, μmol (NO^3+NO^2) L^{-1}) for each station of the Chl *a* dataset was estimated from the nitrate climatology in the World Ocean Atlas 2009 (WOA). We then fitted a model describing the effects of nutrient concentration on NBSS.

2.4. Parameterisation of species size-dependent nutrient resource acquisition and growth rate. The dependence of growth rate (μ) on ambient nutrient concentration is usually modeled using Droop model (Droop, 1973). Aksnes and Egge (1991) developed a theoretical framework that explains how cell size should affect the parameters in Droop model. This theoretical prediction was demonstrated with experimental data by Litchman et al. (2006). Edwards et al. (2012) estimated the allometric parameters for V_{max} (the maximum cell-specific nutrient uptake rate, μmol nutrient $cell^{-1}$ d^{-1}) and K_m that we use here in our model (Fig. 2B):

$$log_{10}(V_{max}) = -8.1 + log_{10}(Vol) \times 0.82 \quad (4)$$

$$log_{10}(K_m) = -0.84 + log_{10}(Vol) \times 0.33 \quad (5)$$

Where Vol is the cell volume (μm^3) and K_m is the nutrient concentration where $V=V_{max}/2$ (Litchman et al., 2009).

To reach an estimate of a relationship between μ and S using Droop model requires the solution of a set of differential equations. Because our intention is only to evaluate the possible effects that a nutrient dependence formulation can have on the determination of community growth rates, we have followed a simpler approach by using relative uptake rate as a proxy for growth rate (Aksnes and Egge, 1991). Hence we have formulated the relative uptake rate (V_{rel}, d^{-1}) as:

$$V_{rel} = \mu_{sp} = V_{max} \frac{S}{Q(K_m + S)} \quad (6)$$

Where μ_{sp} is the growth rate (d^{-1}), the subscript "sp" is used to differentiate the monospecific growth rate (μ_{sp}) from the multispecific community-average growth rate (μ_{com}) as measured in dilution experiments, Q is the cell nutrient content (μmol of nutrient $cell^{-1}$) and V_{max} is the maximum uptake rate constrained by diffusion in the boundary layer outside the cell. In eq. 6, V_{max} and K_m are calculated from cell size using Eqs. 4-5. To estimate Q, we follow Aksnes and Egge (1991) in assuming biomass as the average number of atoms of a given element within the cell, estimated from cell carbon content using a carbon-to-volume ratio ($C:V_{ratio}$) of 0.28 pg C μm^3 based on the empirical equation given in Litchman et al. (2007) and a redfield ratio of 106 C: 16 N.

The implications of these assumptions are evaluated in the discussion.

The community-average growth rate (μ_{com}) as measured in dilution experiments can be calculated from knowledge of the monospecific growth rate for each of the species in the community μ_{sp_i} and the biomass of each species in the community which can be calculated from the numerical abundance times the species cell carbon content. The community biomass at the beginning of the dilution experiment ($B_{initial}$) is:

$$B_i = N_i \times C_i$$

$$B_{initial} = \sum_{n}^{i=1} B_i \qquad (7)$$

Where B_i is the biomass (g C mL^{-1}), N_i is the numerical abundance (cell mL^{-1}) and C_i the cell carbon content (g C $cell^{-1}$) of each species in the community.

At the end of the experiment (assuming a 24 hour experiment in the absence of grazing), the biomass (B_{final}) would be:

$$B_{final} = \sum_{n}^{i=1} (B_i \exp^{\mu_{sp_i} \times t}) \qquad (8)$$

Where t is the duration of experiment (d^{-1}).

The predicted community growth rate is so defined as:

$$\mu_{com} = \frac{\log(B_{final}/B_{initial})}{t} \qquad (9)$$

3. Results

3.1. In situ data - In situ phytoplankton community growth rates (μ_{com}) do not respond to nutrient variation following Monod's kinetics (Fig. 3A). The correlation between in situ μ_{com} and estimated in situ nutrient concentration was non significant ($R^2 = 0.01$, $p = 0.2849$). The response of the growth rate to nutrient concentration is often considered to follow a Monod model when phytoplankton community is limited by nutrient (below 1 μmol L^{-1}). In our dataset, for nutrient concentrations below 1 μmol L^{-1}, in situ phytoplankton community growth rate does not respond to nutrient concentration either ($R^2 = 0.05$, $p = 0.0578$, Fig. 3B). Even if data are corrected for temperature effects (using Arrhenius-Boltzmann equation with activation energy of -0.33 eV, López-Urrutia et al. (2006)), the in situ community growth rate did not follow Monod kinetics (Fig. 4). However, our results show that the in situ μ_{com}:μ_{com_max} ratios (or μ_{com_rel}) do indeed follow a Monod model with $K_s = 0.16 \pm 0.02$ and $\mu_{com\_rel\_max} = 0.99 \pm 0.02$ (Fig. 3C). For nutrient concentration below 1 μmol L^{-1}, in situ μ_{com_rel} also follows Monod's

growth kinetics with $K_s = 0.14 \pm 0.06$ and $\mu_{com\_rel\_max} = 0.91 \pm 0.14$ (Fig. 3D).

3.2. Simulation - A linear model of NBSS v.s nutrient concentration explained 43% of the variance with an increasing size spectra slope (i.e., less negative NBSS) with increasing nutrient concentration (Fig. 2A). Each species composing the simulated phytoplankton community was limited by nutrient and respond to the nutrient concentration following Monod's model. However, the predicted community growth rate ($\mu_{com\_predicted}$) for the simulated communities did not follow Monod kinetics (Fig. 5A). On the contrary, and similar to in situ results, the predicted μ_{com_rel} was well in accordance with Monod's model (Fig. 5B, $K_s = 0.11 \pm 0.01$ and $\mu_{com\_rel\_max} = 0.98 \pm 0.01$).

4. Discussion

In this study, we observed that in situ phytoplankton community growth rate does not respond to nutrient concentration following a Monod kinetic as phytoplankton species composing the community do. However, for the relative reproductive rates, the Monod model is a good characterization of community dynamics.

The lack of significant response following a Monod kinetic may be explained by factors other than nitrate concentration limiting phytoplankton community growth rate. Indeed, we observed that from the total 242 in situ phytoplankton community growth rate data, 110 were from High Nutrient-Low Chlorophyll (HNLC) oceanic regions and so under iron limitation. If the data from HNLC zones are removed from our analysis, we observe that the relationship between phytoplankton community growth rate and nitrate concentration is closer to follow a Monod kinetic than considering the whole dataset ($R^2 = 0.43$, $p < 0.05$). The iron limitation may partly explain the lack of Monod kinetic between the in situ phytoplankton community growth rate and nitrate concentration presented here. However, we observed that in situ phytoplankton community growth rate does not respond to nutrient concentration following a Monod kinetic at nutrient concentrations below 1 μmol L^{-1} although these data do not correspond to iron-limited HNLC regions. The estimation of phytoplankton growth rate by dilution experiments in the most oligotrophic regions may be biased and have to be taken with caution. Indeed, Latasa et al. (2014) explained that most of the studies determining phytoplankton growth rate from dilution experiment presented regression slopes between apparent phytoplankton growth rate and dilution different from zero

when the null hypothesis to be tested in dilution experiment should be the positive slope (b<0) and not a null slope (b=0). Latasa and co-workers believed that a proportion of the experiments with non-significant regressions were disregarded eliminating ecological situations of low growth and grazing. This may result in an overestimation of phytoplankton growth rates.

Although the presented patterns from dilution experiments have to be taken with caution considering the iron limitation at high nutrient concentration and the possible overestimation of phytoplankton growth rate at low nutrient concentration, we observed similar results from in situ phytoplankton community growth rate determined by another methodology. Indeed, we analysed the response of the in situ phytoplankton community growth rate calculated from primary production and standing stocks (Chen and Liu 2010) and nitrate concentration (Fig. 6). As we observed for the dilution experiment, the in situ phytoplankton community growth rate does not respond to nitrate concentration following a Monod kinetic both considering and excluding data from HNLC zones ($R^2 = 0.17$, $p < 0.05$ and $R^2 = 0.06$, $p < 0.05$ respectively). This result confirms our previous observation of the lack of Monod kinetic between in situ phytoplankton community growth rate and nutrient concentration. Unfortunately, the primary production data did not have been analysed under nutrient amended and the maximum growth rate could not have been estimated.

Marine biogeochemical models in use are composed by three or four compartments (i.e. nutrient phytoplankton zooplankton, NPZ or nutrient phytoplankton zooplankton detritus, NPZD) (McCreary et al., 2001; Hood et al., 2003; Kantha, 2004) to 20 or more components including different phytoplankton functional groups, various nutrients and so on (Anderson, 2005; Lancelot et al., 2005; Le Quéré et al., 2005). The NPZ and NPZD models describe a simple food web system assuming dissolved nutrients are consumed by the phytoplankton community following Monod kinetics. For these models, the phytoplankton compartment is considered as a whole community and assumed to respond to nutrient concentration as phytoplankton species do. As we observed in this study, in situ and predicted phytoplankton community do not necessarily respond to nutrient concentration like individual phytoplankton. Thus, marine biogeochemical models using different phytoplankton functional groups (Anderson, 2005; Le Quéré, 2005) or based on phytoplankton size structure (Follows et al., 2007; Edwards et al., 2012) should rather be used instead of simpler models as NPZ or NPZD. This is well in line to the findings of Friedrichs et al. (2006; 2007) that

observed that complex models with multiple phytoplankton functional groups fit better the available data than the simpler models. This is mainly due to the use of many tuning parameters and thus degrees freedom. The parameterization of planktonic ecosystem models should not use the same variables for a community than for species. Franks (2009) warned about the use of community variables parameterized using data from individual species and suggested that the response to nutrient concentration of an individual or species should not represent necessarily the response of a diverse community. Contrary to our results, Franks (2009) observed a linear relation between the community nutrient uptake rate and nutrient concentration that could be explained by the use of the same half-saturation constant (K_s) for all phytoplankton size classes in his simulations. Several published works reported that K_s is different between species (Sommer, 1991; Chisholm, 1992; Cermeño et al., 2011). In our study, the relationship between the in situ community growth rate and nutrient concentration did not follow a Monod kinetic, neither a linear relationship.

Many models (e.g. Darwin model) use a trade-off between K_s and μ_{max}—some organisms grow fast at high nutrient concentrations (high V_{max} or μ_{max}) and others may be better competitors at low nutrient concentrations with low K_s. Without this trade-off, small phytoplankton would outcompete large phytoplankton in the whole ocean unless other constrains are introduced (e.g. top-down differences). Although this trade-off would maintain species coexistence in a competition model, this theoretical perspective is in contrast with the empirical evidence on the size dependence of K_s and μ_{max}. Indeed, the most up-to-date compilations on the size dependence of K_s and μ_{max} do not reveal the existence of a trade-off between these two variables. Edwards et al. (2012) found that K_s increases with increasing cell size and V_{max} and μ_{max} decrease with increasing size. Furthermore, Fiksen et al. (2013) were unable to identify any mechanistic trade-off conflicts between K_s and V_{max}. In this work, we decided to parameterize empirical phytoplankton growth rate and size (Fig. 1) without accounting the trade-off between K_s and μ_{max} considering that recent empirical data do not reveal its existence.

Several studies have shown that the high surface area to volume (S:V) ratio of small phytoplankton species result in high maximum nutrient uptake rates and low K_s and may explain why small phytoplankton species dominate in natural nutrient-limited ecosystems (Eppley et al., 1969; Aksnes and Egge, 1991; Hein et al., 1995). Conversely, large phytoplankton species seem to dominate in productive and well-

285 mixed ecosystems (Irwin et al., 2006) due to their physical and chemical capacities to
286 escape to zooplankton grazing (Irigoien et al., 2004; Irigoien et al., 2005) and due to
287 upward motion increasing their residence time in upper layer against their tendency to
288 sink (Li, 2002; Rodríguez et al., 2001). Furthermore, allometric equations explain that
289 small phytoplankton species achieves higher growth rate than a large phytoplankton
290 species at a same nutrient concentration (Edwards et al., 2012). Considering the
291 allometric equations and the low nutrient-small phytoplankton and high nutrient-large
292 phytoplankton relations, the community growth rate can be higher at low than at high
293 nutrient concentration. We observed in this study that most of the community growth
294 rates tended to decrease from 5 to 30 mmol NO^3+NO^2 m^{-3} (Fig. 3A) for the in situ data
295 (R^2 = 0.15, p < 0.001) and from 2.5 to 25 mmol NO^3+NO^2 m^{-3} (Fig. 5A) for the
296 predicted data (R^2 = 0.17, p < 0.001). Therefore, our results support our hypothesis of
297 higher community growth rates at intermediate than at the highest nutrient
298 concentrations.

299 In our simulation, we assumed that the intrinsic nutrient storage is related to the
300 growth rate and ignored, for the sake of simplicity in the simulations the cell storage
301 capacity. Indeed, Litchman et al. (2009) observed that when nitrogen supply is pulsed,
302 large cells could dominate due to their enhanced storage capacities. By this observation,
303 we should expect to observe higher growth rates for large phytoplankton species at high
304 nutrient concentration than for small phytoplankton species, but if so a better
305 relationship between community growth rate and nutrient concentration would be
306 expected. The relationship between μ_{sp_max} and cell volume might influence the kinetic
307 of the community growth rate response to nutrient concentration. Although there is
308 consensus on the fact that smaller cells have lower half-saturation constants, the
309 relationship between μ_{sp_max} and cell size is still under debate (Chen and Liu, 2011; Sal
310 and López-Urrutia, 2011). Two different relations have been observed between
311 μ_{sp_max} and cell volume: unimodal (Bec et al., 2008; Chen and Liu, 2011; Marañon et
312 al., 2013) and declined lineal (Edwards et al. 2012). In addition, the parameterizations
313 of some models argue for an increased lineal relationship (Follows et al., 2007). To
314 understand the consequences of different relationships between μ_{sp_max} and cell size, we
315 repeated our simulations but using unimodal (Fig. 7A) and positive (Fig. 7B)
316 relationships between μ_{sp_max} and cell size. We observed that when the relation between
317 μ_{sp_max} and cell volume is unimodal, the predicted community growth rates did not

follow Monod's kinetic either (Fig. 7A). When the relation between μ_{sp_max} and cell volume is positive (i.e., larger cells have higher $\mu_{sp\text{-}max}$), the model output suggests a possible relation between the predicted community growth rates and nutrient concentration (Fig. 7B). Hence, the observed lack of relationship in the in situ data (Fig. 3A) could be reproduced with the unimodal but not with the positive relationship.

Although community growth rates did not respond to nutrient concentration following Monod kinetics, the in situ and simulated μ_{com_rel} did (Fig.s 3B, 5B). The μ_{com_rel} is exempted from the effects of temperature, light and community composition. The K_s and $\mu_{com\_rel\_max}$ were quite similar between the in situ (K_s = 0.16 ± 0.02 and $\mu_{com\_rel\_max}$ = 0.99 ± 0.02) and predicted (K_s = 0.11 ± 0.01 and $\mu_{com\_rel\_max}$ = 0.98 ± 0.01) μ_{com_rel}. So when the community growth rate depends only on nutrient concentration, the response of the community growth rate to nutrient variation follows the predicted Monod kinetic.

In summary, our study demonstrates that the lack of relationship between community growth rates and nutrients can be explained even if we disregard the effects of temperature, light or community composition. We could expect that such factors might further distort the observed relationship between the community growth rate and nutrient concentration.

Acknowledgment

This work was supported by Metabolic Ocean Analysis (METOCA) funded by Spanish National Invsetigation+Development+Innovation (I+D+I) Plan. We thank E. Marañon for sharing his phytoplankton size structure data and Ángel Segura for his useful comments and corrections. This is a contribution to times series project RADIALES from the Instituto Español de Oceanografía (IEO).

References

Agustí, S., Duarte, C .M., and Kalff, J.: Algal cell size and the maximum density and biomass of phytoplankton, Limnol. Oceanogr., 32, 983-986, 1987.

Aksnes, D. L., and Egge, J. K.: A theoretical model for nutrient uptake in phytoplankton, Mar. Ecol. Prog. Ser., 70, 65-72, 1991.

Anderson, T. R.: Plankton functional type modeling: running before we can walk?, J. Plankton Res., 27, 1073– 1081, doi:10.1093/plankt/fbi076, 2005.

Bec, B., Collos, Y., Vaquer, A., Mouillot, D., and Souchu, P.: Growth rate peaks at intermediate cell size in marine photosynthetic picoeukaryotes, Limnol. Oceanogr., 53, 863-867, 2008.

Brown, S. L., Landry, M. R., Christensen, S., Garrison, D., Gowing, M. M., Bidigare, R. R., and Campbell, L.: Microbial community dynamics and taxon-specific phytoplankton production in the Arabian Sea during the 1995 monsoon seasons, Deep-Sea Res., 49, 2345-2376, 2002.

Cermeño, P., Lee, J.-B., Wyman, K., Schofield, O., and Falkowski, P. G.: Competitive dynamics in two species of marine phytoplankton under non-equilibrium conditions, Mar. Ecol. Prog. Ser., 429, 19-28, 2011.

Chen, B. Z., and Liu, H. B.: Relationships between phytoplankton growth and cell size in surface oceans: Interactive effects of temperature, nutrients, and grazing, Limnol. Oceanogr., 55, 965-972, 2010.

Chen, B. Z., and Liu, H. B.: Comment: Unimodal relationship between phytoplankton-mass-specific growth rate and size: A reply to the comment by Sal and López-Urrutia (2011), Limnol. Oceanogr., 56, 1956-1958 2011.

Chisholm, S. W.: Phytoplankton size, in: Primary productivity and biogeochemical cycles in the sea, Plenum Press, Falkowski, P. G. and Woodhead, A. D., 213-237, 1992.

Dugdale, R. C.: Nutrient limitation in the sea: dynamics, identification, and significance, Limnol. Oceanogr., 12, 685-695, 1967.

Edwards, K. F., Thomas, M. K., Klausmeier, C. A., and Litchman, E.: Allometric scaling and taxonomic variation in nutrient utilization traits and maximum growth rate of phytoplankton, Limnol. Oceanogr., 57, 554-566, 2012.

Eppley, R. W., Rogers, J. N., and McCarthy, J. J.: Half-saturation constants for uptake of nitrate and ammonium by marine phytoplankton, Limnol. Oceanogr., 14, 912-920, 1969.

Follows, M. J., S., Dutkiewicz, S., Grant, and S. W. Chisholm. 2007. Emergent biogeography of microbial communities in a model ocean. Science 315: 1843-1846.

Franks, P. J.: Planktonic ecosystem models: Perplexing parameterizations and a failure to fail, J. Plankton Res., 31, 1299-1306, 2009.

Friedrichs, M. A. M., Hood, R., and Wiggert, J.: Ecosystem model complexity versus physical forcing: Quantification of their relative impact with assimilated Arabian Sea data, Deep Sea Res. II, 53, 576– 600, 2006.

Friedrichs, M. A. M., Dusenberry, J. A., Anderson, L. A., Armstrong, R. A. A., and Chai, F.: Assessment of skill and portability in regional marine biogeochemical models: Role of multiple planktonic groups, J. Geophys. Res., 112, doi: 10.1029/2006JC003852, 2007.

Grover, J. P.: Influence of cell shape and size on algal competitive ability, Am. Nat., 138, 811-835, 1989.

Hein, M., Pedersen, M. F., and Sand-Jensen, K.: Size-dependent nitrogen uptake in micro- and macroalgae, Mar. Ecol. Prog. Ser., 118, 247-253, 1995.

Hillebrand, H., Dürselen, C.-D., Kirschtel, D., Pollinger, U., and Zohary, R.: Biovolume calculation for pelagic and benthic microalgae, J. Phycol., 35, 403-424, 1999.

Hood, R. R., Kohler, K. E., McCreary, J. P., and Smith, S. L.: A fourdimensional validation of a coupled physical-biological model of the Arabian Sea, Deep Sea Res. II, 50, 2917– 2945, 2003.

Irigoien, X., Huisman, J., and Harris. R. P.: Global biodiversity patterns of marine phytoplankton and zooplankton, Nature, 429, 863-867, 2004.

Irigoien, X., Flynn, K. J., and Harris, R. P.: Phytoplankton blooms: A 'loophole' in microzooplankton grazing impact?, J. Plankton Res., 27, 313-321, 2005.

Irwin, A. J., Finkel, Z. V., Schofield, O. M. E., and Falkowski, P. G.: Scaling-up from nutrient physiology to the size-structure of phytoplankton communities, J. Plankton Res., 28, 459-471, 2006.

Kantha, L. H.: A general ecosystem model for applications to studies of carbon cycling and primary productivity in the global oceans. Ocean Modell, 6, 285– 334, 2004.

Lancelot, C., Spitz, Y., Gypens, N., Ruddick, K., Becquevort, S., Rousseau, V., Lacroix, G., and Billen, G.: Modelling diatom-Phaeocystis blooms and nutrient cycles in the Southern Bight of the North Sea: The MIRO model, Mar. Ecol. Prog. Ser., 289, 63–78, 2005.

Landry, M. R., and Hassett, R. P.: Estimating the grazing impact f marine micro-zooplankton, Mar. Biol., 67, 283-288, 1982.

Le Quéré, C., Harrison, S. P., Prentice, I. C., Buitenhuis, E. T., Aumont, O., Bopp, L., Claustre, H., Cotrim Da Cunha, L., Geider, R., Giraud, X., Klaas, C., Kohfeld, K. E., Legendre, L., Manizza, M., Platt, T., Rivkin, R. B., Sathyendranath, S., Uitz, J., Watson, A. J., and Wolf-Gladrow, D.: Ecosystem dynamics based on plankton functional types for global ocean biogeochemistry models. Global Change Biol., 11, 2016–2040, 2005.

Li, W. K. W.: Macroecological patterns of phytoplankton in the northwestern North Atlantic Ocean, Nature, 419, 154-157, 2002.

Litchman, E., Klausmeier, C. A., Miller, J. R., Schofield, O. M., and Falkowski, P. G.: Multi-nutrient, multi-group model of present and future oceanic phytoplankton communities, Biogeosciences, 3, 607-663, 2006.

Litchman, E., Klausmeier, C. A., Scholfield, O. M., and Falkowski, P. G.: The role of functional traits and trade-offs in structuring phytoplankton communities: scaling from cellular to ecosystem level, Ecol. Lett., 10, 1-12, 2007.

Litchman, E., Klausmeier, C. A., and Yoshiyama, K.: Contrasting size evolution in marine and freshwater diatoms, P. Natl. Acad. Sci., 106, 2665-2670, 2009.

López-Urrutia, A., San Martin, E., Harris, R. P., and Irigoien, X.: Scaling the metabolic balance of the oceans, P. Natl. Acad. Sci. USA., 103, 8739-8744, 2006.

Marañón, E., Cermeño, P., Latasa, M., and Tadonléké, R. D.: Termperature, resources, and phytoplankton size structure in the ocean, Limnol. Oceanogr., 57, 1266-1278, 2012.

Marañon, E., Cermeño, P., López-Sandoval, D. C., Rodríguez-Ramos, T., Sobrino, C., Huete-Ortega, M., Blanco, J. M., and Rodríguez, J.: Unimodal size scaling of phytoplankton growth and the size dependence of nutrient uptake and use, Ecol. Lett., 16, 371-379, 2013.

McCreary, J. P., Kohler, K. E., Hood, R. R., Smith, S., Kindle, J., Fischer, A. S., and Weller, R. A.: Influences of diurnal and intraseasonal forcing on mixed-layer and biological variability in the central Arabian Sea, J. Geophys. Res., 106, 7139–7155, 2001.

Partensky, F., Hess, W. R., and Vaulot, D.: Prochlorococcus, a marine photosynthetic prokaryote of global significance, Microbiol. Mol. Biol. R., 63, 106-127, 1999.

Rodríguez, J., Tintoré, J., Allen, J. T., Blanco, J. M., Gomis, D., Reul, A., Ruíz, J.,

Rodríguez, V., Echevarría, F., and Jiménez-Gómez, F.: Mesoscale vertical motion and the size structure of phytoplankton in the ocean, Nature, 410, 360-363, 2001.

Sal, S., and López-Urrutia, Á.: Comment: Temperature, nutrients, and the size-scaling of phytoplankton growth in the sea, Limnol. Oceanogr., 56, 1952-1955, 2011.

Sommer, U.: A comparison of the Droop and the Monod models of nutrient limited growth applied to natural populations of phytoplankton, Funct. Ecol., 5, 535-544, 1991.

Sprules, W. G., and Munawar, M.: Plankton size spectra in relation to ecosystem productivity, size, and perturbation, Can. J. Fish. Aquat. Sci., 43, 1789-1794, 1986.

Tremblay, J.-E., and Legendre, L.: A model for the size-fractionated biomass and production of marine phytoplankton, Limnol. Oceanogr., 39, 2004-2014, 1994.

Figure Legends

Figure 1. Conceptual diagram representing phytoplankton communities composed by small and large phytoplankton species (small grey and large black circles, respectively) in nutrient-limited and productive ecosystems. Each phytoplankton species composing their respective communities had is own growth rate response to nutrient concentration following a Monod kinetic. The growth rates for the whole community in both ecosystems have been evaluated by the mean of the cell-specific growth rates of each phytoplankton species composing their respective communities. At the bottom of the diagram, community growth rates for both ecosystems are represented at specific nutrient concentrations.

Figure 2. Functional forms of (A) normalized biomass spectrum (NBSS) and (B) phytoplankton species growth rate to nutrient concentration. (B) Simple allometric equations are indicated by the size range from small (thinnest lines) to large (thickest lines) size species. (A) The solid line represents the linear regression.

Figure 3. Relationships between in situ community growth rate (μ_{com}, d^{-1}) and nutrient concentration (A) from 0 to 40 mmol m^{-3} and (B) from 0 to 1 mmol m^{-3}. Relationships between in situ μ_{com}:μ_{com_max} ratio and nutrient concentration (C) from 0 to 40 mmol m^{-3} and (D) from 0 to 1 mmol m^{-3}. Crosses represent phytoplankton communities of Table A1 sampled in HNLC regions (High-Nutrient, Low-Chlorophyll) and circles represent the rest of the phytoplankton communities from Table A1 dataset. (C, D) The solid lines represent the nonlinear least square fits for the global dataset (HNLC included).

Figure 4. Relationship between in situ community growth rates ($\mu_{com}e^{Ea/KT}$, d^{-1}) corrected by temperature using the average activation energy for autotrophic respiration (Ea = -0.33 eV, López-Urrutia et al. (2006)) and nitrate concentration (mmol m^{-3}). Crosses represent phytoplankton communities of Table A1 sampled in HNLC regions (High-Nutrient, Low-Chlorophyll) and circles represent the rest of the phytoplankton communities from Table A1 dataset.

Figure 5. Relationships between (A) predicted community growth rate ($\mu_{com\_predicted}$, d^{-1}) and (B) predicted μ_{com}:μ_{com_max} ratio, and nutrient concentration (mmol m^{-3}). The solid

lines represent the nonlinear least square fits.

Figure 6. Relationships between in situ community growth rates (μ_{PP}, d^{-1}) estimated from primary production and standing stocks and nitrate concentration (A) from 0 to 40 mmol m^{-3} and (B) from 0 to 1 mmol m^{-3} from Chen and Liu (2) Table A2 dataset. Crosses represent phytoplankton communities of Table A2 sampled in HNLC regions (High-Nutrient, Low-Chlorophyll) and circles represent the rest of the phytoplankton communities from Table A2 dataset.

Figure 7. Relationships between the predicted community growth rates ($\mu_{com\_predicted}$, d^{-1}) and nitrate concentration (mmol m^{-3}) with (A) unimodal and (B) positive relationships between μ_{com_max} and cell size.

502 **Figure 1.**

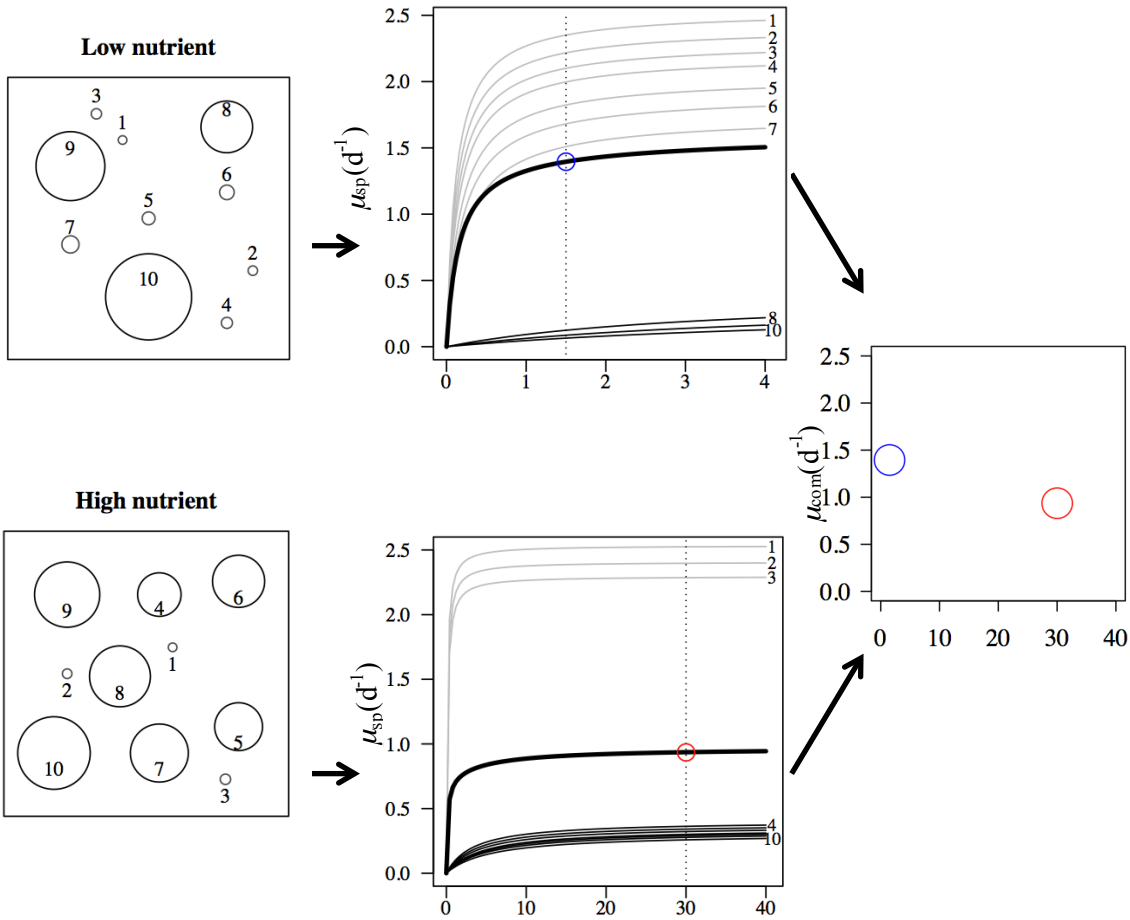

503

Figure 2.

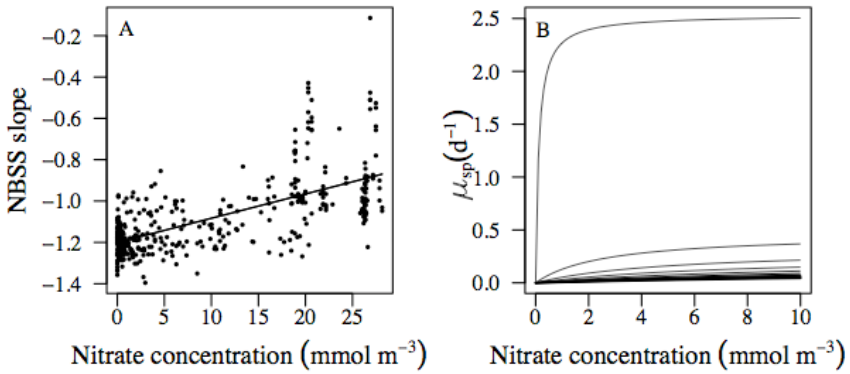
A
NBSS slope
−0.2
−0.4
−0.6
−0.8
−1.0
−1.2
−1.4
0
5
10
15
20
25
Nitrate concentration (mmol m^{-3})
B
μ_{sp}(d^{-1})
2.5
2.0
1.5
1.0
0.5
0.0
0
2
4
6
8
10
Nitrate concentration (mmol m^{-3})

Figure 3.

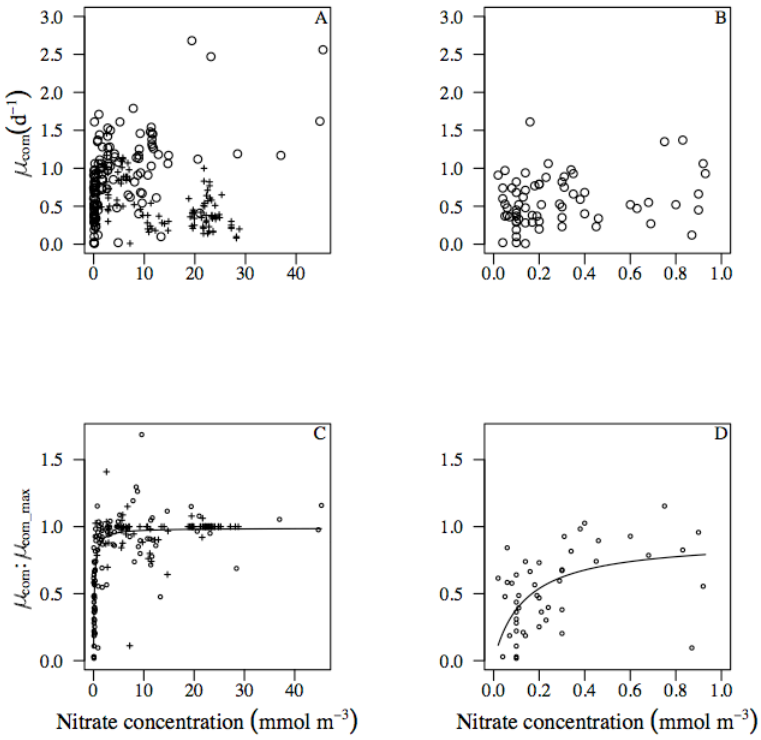
A
B
C
D
μ_{com} (d^{-1})
μ_{com} : μ_{com_max}
Nitrate concentration (mmol m^{-3})
Nitrate concentration (mmol m^{-3})

508 **Figure 4.**

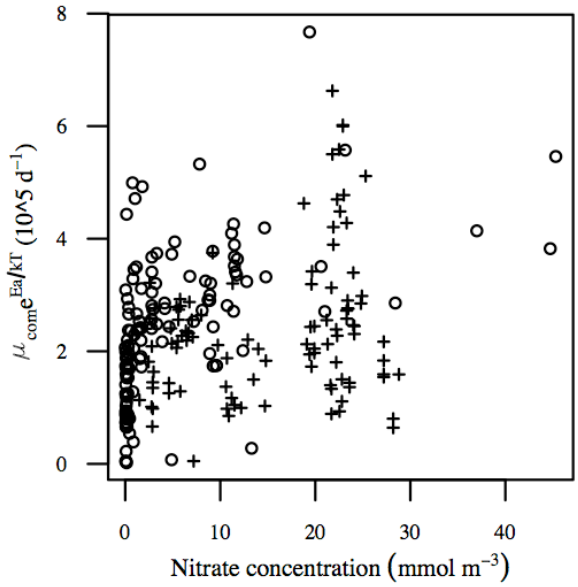
8
6
4
2
0
$\mu_{com}e^{Ea/kT}$ (10^5 d^{-1})
0
10
20
30
40
Nitrate concentration (mmol m^{-3})

509 **Figure 5.**

510

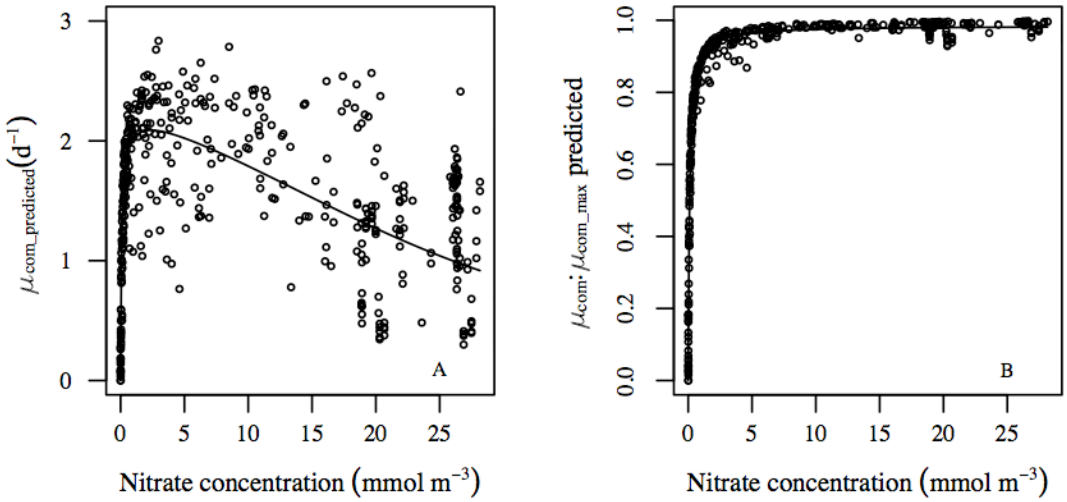

Figure 6.

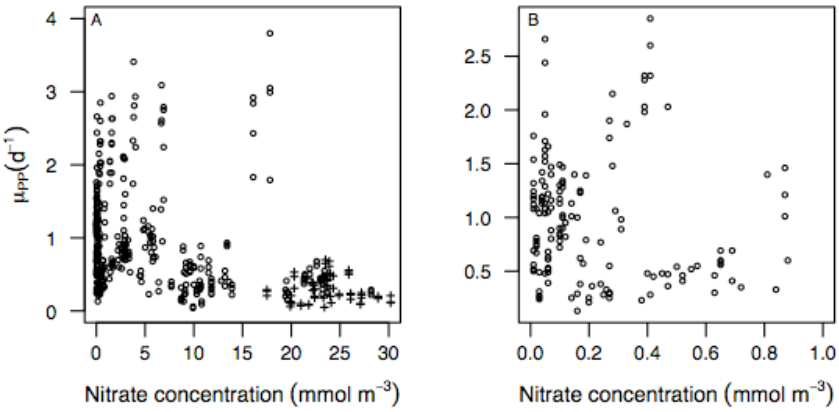
A
B
$\mu_{PP}(d^{-1})$
Nitrate concentration (mmol m^{-3})
Nitrate concentration (mmol m^{-3})

514 **Figure 7.**

515

516